Process Safety and Environmental Protection 105 (2017) 316–325

Contents lists available at ScienceDirect

Process Safety and Environmental Protection

journal homepage: www.elsevier.com/locate/psep

The feasibility of *Thamnidium elegans* cells for color removal from real wastewater

Tamer Akar[a,*], *Fatih Sayin*[a], *Serpil Turkyilmaz*[b], *Sibel Tunali Akar*[a]

[a] *Department of Chemistry, Faculty of Arts and Science, Eskişehir Osmangazi University, Turkey*
[b] *Department of Statistics, Faculty of Arts and Science, Bilecik Şeyh Edebali University, 11210 Bilecik, Turkey*

ARTICLE INFO

Article history:
Received 3 October 2016
Received in revised form 11 November 2016
Accepted 17 November 2016
Available online 24 November 2016

Keywords:
Biosorption
Dye
Process design
Reactive Yellow 2 (RY2)
Real wastewater
Thamnidium elegans

ABSTRACT

Biosorptive treatment of contaminated solutions with different biomaterials has been extensively studied in recent years. However, application of the suggested biosorbents in industrial scale has been very limited so far. Real wastewater conditions play an important role in the commercial success of the biosorption process. This study describes the potential use of *Thamnidium elegans* (*T. elegans*) cells for the biosorptive treatment of real industrial wastewater. Biosorption mechanism was characterized by zeta potential, Brunauer, Emmett and Teller (BET), Infrared (IR) spectrometry, Atomic force microscopy (AFM) and elemental analysis. A quadratic model was built for the batch process and optimum values of variables were recorded as pH 2.0, biosorbent amount: 0.06 g and contact time: 39.3 min with the removal yield of 99.42%. Isotherm studies indicated that the process follows the Langmuir model. Relatively fast decolorization (40 min) process was well described by the pseudo-second-order kinetics. Conversely, the biosorbent exhibited high biosorption efficiency (97.55%) in continuous mode. In addition to high batch biosorption capacity (288.08 mg g^{-1}) of the biosorbent, another impressive aspect of this study, even after ten regeneration cycles, is high biosorption yield (95%). Consequently, *T. elegans* cells showed great potential for the treatment of colored real wastewaters.

1. Introduction

In recent years, the removal of synthetic dyes from contaminated aquatic media has received great attention in the field of environmental studies. They are toxic for living organisms, cause to aesthetic problem in water sources and have negative effects on bacterial growth and photosynthetic activities of aquatic plants (Allen and Koumanova, 2005). The degradation of dye molecules in the contaminated media is very difficult because of their complex and stable molecular structure. Besides, reductive cleavage of azo linkages in the dye structure can produce toxic and carcinogenic amine compounds (Solís et al., 2012). Therefore, environmentally friendly and economical treatment methods are required for the removal of synthetic dyes from industrial effluents and other contaminated waters.

Recent investigations related to environmental technology have focused on the use of biosorption method for decolorization of contaminated aquatic media (Tunali Akar et al., 2011; Akar et al., 2016; Lee et al., 2016; Fontana et al., 2016; Fernandez et al., 2012; Daneshvar et al., 2017; Nath et al., 2016). This physicochemical technology generally utilizes non-living cells of biomaterials such as fungi, algae and bacteria to sequester synthetic dyes and other water contaminants. Chitin, glucan, protein, mannan, melanine and lipid fractions of the microbial cells can provide potential binding sites for pollutants (Fomina and Gadd, 2014).

The cost of the biosorbent materials used in the biosorptive treatment of contaminated waters is competitive with that of the conventional sorbents. In this process, biosorbent can be produced by unsophisticated fermentation techniques in addition to evaluation of the by-products of large-scale fermentations such as enzyme

* *Corresponding author at*: Department of Chemistry, Faculty of Arts and Science, Eskişehir Osmangazi University, Campus of Meşelik, 26480 Eskişehir, Turkey. Fax: +90 222 2393578.
E-mail address: takar@ogu.edu.tr (T. Akar).
http://dx.doi.org/10.1016/j.psep.2016.11.017

and pharmaceutical production (Kuyucak, 1990). The efficiency of the biosorptive decolorization process depends on various factors such as solution pH, biomaterial dosage and time. The interactive effects of considered process variables on the biosorption process are not evaluated with the classical optimization approach which based on "ovat (one-variable-a-time)" approach. On the other hand, the application of the statistical experimental design based on the response surface methodology (RSM) to biosorption process allowed to systematic, efficient and simultaneous analysis of control variables (Hasan et al., 2009).

Although large number of decolorization studies have been carried out with synthetic dye solutions, the other organic and inorganic species present in industrial wastewater medium can significantly effect the biosorption performance of biomaterials. In order to transfer the findings from laboratory scale to real applications there is a need to generate relative performance data on real industrial wastewater conditions. The current biosorption applications are still insufficient to cover the problem of the pollutant removal from real industrial wastewaters (Vijayaraghavan and Yun, 2008a; Tigini et al., 2011).

Organic pollutants such as synthetic dyes can be effectively removed by adsorption onto activated carbon. But relatively high operation cost restricts its large-scale application. Therefore, different low-cost sorbent materials have been examined for the treatment of wastewater. A zygomycete strain *Thamnidium elegans* (*T. elegans*) can produce substantial amount of biomass in unsophisticated liquid culture medium. So it can be used as adsorbent instead of commercial activated carbon. γ-Linolenic acid production in solid state fermentation conditions (Stredansky et al., 2000), bioconversions of rapamycin (Kuhnt et al., 1997) and waste glycerol (Chatzifragkou et al., 2011), are reported applications of this fungal strain. Although our recent findings based on the classical optimization method indicated that *T. elegans* cells have a great biodecolorization potential (Akar et al., 2013a,b), the batch mode biosorption characteristics of *T. elegans* cells for a pollutant based on the statistical experimental design methodology and its real wastewater treatment potential were examined for the first time. Hence, the goal of the present study was to suggest an efficient biomaterial for the treatment of the real industrial wastewater and to improve the performance of the decolorization process by *T. elegans*. Response surface methodology (RSM) was firstly employed using Box Behnken surface design to identify the interactive and individual effects of Reactive Yellow 2 (RY2) decolorization by *T. elegans*. In addition to systematic variation of the parameters, process was modeled by isotherm and kinetic approaches. Pollutant–biomass interactions in the process were assisted by using BET, IR, AFM and elemental analysis. The regenerable biomass was also effectively used in the dynamic flow treatment mode.

2. Materials and methods

2.1. Biosorbent

T. elegans (ATCC 18191) was grown and harvested according to procedure reported in our previous studies (Akar et al., 2013a,b). Harvested biomass was repeatedly washed with deionized water, dried at 60 °C overnight, ground and sieved to particle size of 212 μm. Obtained biomass was kept in a dark glass bottle for further use in the decolorization experiments.

2.2. Dye solutions

RY2 (chemical formula: $C_{25}H_{18}Cl_3N_9O_{10}S_3{\cdot}3Na$; λ_{max}: 396 nm) was selected as model sorbate in real wastewater. Biosorption experiments were performed using real wastewater obtained from a wastewater treatment plant in organized industrial area of Eskişehir (Turkey). The chemical composition of the wastewater was analyzed by AAS (Perkin Elmer Analyst 400) and ion chromatography equipment (Dionex ICS-3000). The concentrations of calcium (Ca^{2+}), magnesium (Mg^{2+}), sodium (Na^{+}), potassium (K^{+}), copper (Cu^{2+}), manganese (Mn^{2+}), chloride (Cl^{-}), sulfate (SO_4^{2-}), nitrate (NO_3^{-}), fluoride (F^{-}), bromide (Br^{-}) and phosphate (PO_4^{3-}) ions were 162.46, 44.01, 863.50, 21.19, 0.10, 0.15, 87.55, 381.75, 1306.35, 0.58, 0.35 and 2.13 mg L^{-1}, respectively. Chemical oxygen demand (COD) of the wastewater was measured as 828.0 mg L^{-1}.

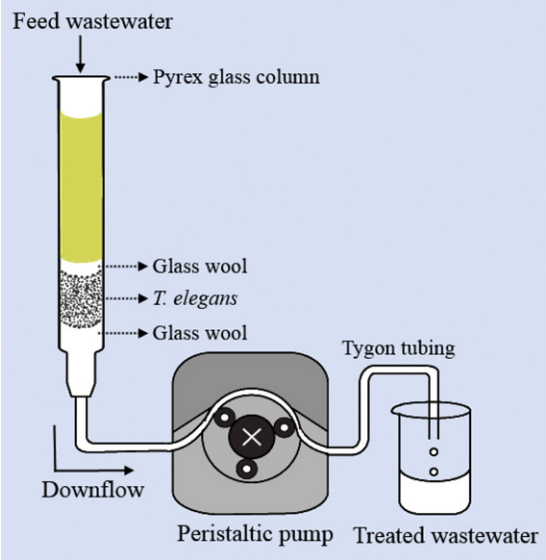

Scheme 1 – Column mode experiments for the biosorption of RY2 onto *T. elegans*.

A series of working solutions at various concentration range were prepared by diluting a stock solution with a concentration of 1000 mg L^{-1}. pH of the working solutions was measured by a pH meter (WTW Inolab 7110) and adjusted to desired values using dilute HNO_3 or NaOH solutions.

2.3. Biosorption experiments

The biosorption performance of the biosorbent in this study was tested in both batch and column modes. The batch mode biosorption studies were conducted by stirring known amount of biosorbent material with 25 mL of dye solution by varying pH, biosorbent amount, contact time and initial RY2 concentration. The effects of these parameters on the biosorption yield of the biosorbent were investigated. After the biosorption, the biosorbent was separated from the liquid phase by centrifugation and the residual concentration of dye in the supernatant was determined by an UV/vis spectrophotometer (Shimadzu UV-2550).

Column biosorption studies were carried out using packed bed glass columns with 9 mm internal diameter (i.d.). Sorbate was passed through the column with a peristaltic pump (Ismatec ecoline) connected with tygon tubings (Scheme 1). Flow rate of sorbate was optimized by changing the flow rate from 0.25 to 2.00 mL min^{-1}. These experiments were conducted using 100 mg L^{-1} dye solutions and 40 mg of biosorbent. Desorption potential of the biosorbent and the breakthrough profile were also evaluated to test the biosorption performance of the biosorbent in real conditions.

2.4. Characterization studies

2.4.1. BET surface area

BET surface area of the biosorbent was determined from N_2 adsorption isotherm with a surface area and pore size analyzer (Quantachrome Instruments, Autosorb 1).

2.4.2. IR analysis

In order to identify the functional groups present on the biosorbent surface, IR spectroscopic analysis was used. Therefore, IR spectra were recorded in the wavenumber range of 4000–400 cm^{-1} using Bruker Tensor 27 FTIR spectrophotometer.

2.4.3. AFM analysis

Atomic Force Microscope (AFM) analysis was used for topographical investigation of biomaterial. Specimens were suspended in sterile distilled water, fixed on a thin glass plate and dried in air at 25 °C. The surface of biomaterials was viewed using Park Systems XE-100-E AFM. Imaging was carried out using non-contact imaging mode, at 300 kHz frequency and 0.9 Hz scan rate in air at room temperature. The spring constant of silicon cantilever was 40 N/m.

2.5. RSM and statistical analysis

The objective of RSM is to develop an emprical model for designing experiments and to optimize the responses influenced by various factors (Chaudhary and Balomajumder, 2014; Fakhri, 2015; Murugesan et al., 2014). In this study Box–Behnken design (BBD) of RSM was selected to design and to analyze the experimental results using Design Expert 7.0 software version. The effects of three variables mainly pH (x_1), biosorbent amount (x_2) and contact time (x_3) on one response (biosorption yield, %) were studied and the variable levels are given in SM1.

In this study, required numbers of the experiment were calculated as follows:

$$N = 2k*(k-1) + cp, \tag{1}$$

where, k is the number of factor, cp is the replicate number of the central point. A system with three independent variables (factors) (x_1, x_2, x_3) and the response variable (Y) can be represented by a quadratic equation;

$$Y = \beta_0 + \beta_1 x_1 + \beta_2 x_2 + \beta_3 x_3 + \beta_{12} x_1 x_2 + \beta_{13} x_1 x_3 + \beta_{23} x_2 x_3 + \beta_{11} x_1^2 + \beta_{22} x_2^2 + \beta_{33} x_3^2 \tag{2}$$

where Y is the response variable (biosorption yield of RY2),

Actual design matrix of total 17 biosorption experiments is also presented in SM2. The fitting of the quadratic model was determined by the coefficient of determination, R^2.

2.6. Biosorption kinetics

In order to determine the kinetic parameters of RY2 biosorption, various kinetic models such as Lagergren's pseudo-first-order (Lagergren, 1989) and the pseudo-second-order (Ho, 2006) kinetic models were adopted. Lagergren's kinetic equation is given below:

$$\ln(q_e - q_t) = \ln q_e - k_1 t \tag{3}$$

which k_1 is pseudo-first-order rate constant (min^{-1}), q_e and q_t are biosorption capacities at equilibrium and at time t ($mg\,g^{-1}$), respectively.

The pseudo-second-order rate equation;

$$\frac{t}{q_t} = \frac{1}{k_2 q_e^2} + \frac{1}{q_e} t \tag{4}$$

k_2 is the pseudo-second-order rate constant ($g\,mg^{-1}\,min^{-1}$).

2.7. Equilibrium studies

Widely used isotherm models i.e. Langmuir, Freundlich and Dubinin–Radushkevich (D–R) were employed to investigate the equilibrium data. Langmuir isotherm (Langmuir, 1918) is expressed by the following equation:

$$\frac{1}{q_e} = \frac{1}{q_{max}} + \left(\frac{1}{q_{max} K_L}\right) \frac{1}{C_e} \tag{5}$$

where q_e is biosorption capacity of the biosorbent at equilibrium ($mol\,g^{-1}$), C_e is the dye concentration in solution at equilibrium ($mol\,L^{-1}$) and K_L is Langmuir equilibrium constant ($L\,g^{-1}$).

The Langmuir isotherm may be expressed by R_L value, a dimensionless constant, referred to as separation factor (Hall et al., 1966):

$$R_L = \frac{1}{1 + K_L C_o} \tag{6}$$

R_L values indicate the biosorption reaction favorable or unfavorable as shown below:

$R_L > 1$, unfavorable
$R_L < 0$, unfavorable
$R_L = 1$, favorable (linear)
$0 < R_L < 1$, favorable
$R_L = 0$, irreversible

The Freundlich isotherm (Freundlich, 1906) is given in Eq. (7) and assumes that biosorption takes place on heterogeneous surfaces.

$$\ln q_e = \ln K_F + \frac{1}{n} \ln C_e \tag{7}$$

where K_F ($L\,mg^{-1}$) is the Freundlich constant and n is the heterogeneity factor.

D–R isotherm model (Dubinin and Radushkevich, 1947) is used to estimate the biosorption energy in order to determine the physical or chemical biosorption mechanism

$$\ln q_e = \ln q_m - \beta \varepsilon^2 \tag{8}$$

$$\varepsilon = RT \ln(1 + 1/C_e) \tag{9}$$

$$E = 1/(2\beta)^{1/2} \tag{10}$$

where q_m is the biosorption capacity ($mol\,g^{-1}$), β is the activity coefficient related to the biosorption energy, E ($kJ\,mol^{-1}$) is the mean free energy.

3. Results and discussion

3.1. Estimation of RSM for maximum RY2 biosorption

In the present study, 3-level and 3-factor Box–Behnken experimental design is applied to investigate the biosorption process variables. 17 experimental runs including 5 replications at the center points were carried out. −1, 0 and +1 are the

coded values of the low, center and high levels for each factor variable, respectively. Uncoded forms of the low and high values for the experimental design are pH 2 and 8, biosorbent amount = 0.02 g and 0.10 g and time = 5 min and 40 min, respectively. Observed results of experimental runs and their predicted values are included in SM1. Observed and predicted values in SM1 are very close and quadratic model was found to be fitted the experimental data for RY2 biosorption on *T. elegans*.

Analysis of Variance (ANOVA) was used to evaluate the statistical significance of the quadratic model and the results are presented in SM2. According to multiple regression analysis in SM2, an empirical relationship between the effective factor variables and the response variable in coded units can be expressed by the following model;

$$\text{RY2 biosorption yield (\%)} = 68.80 - 17.96x_1 + 1075.01x_2 \quad (11)$$

The regression model indicated a high correlation between the predicted and observed values for the biosorption of RY2 on *T. elegans* with a determination coefficient (R^2) of 0.986. A large *F* value of 56.90 showed the regression equation can explain the most of the variation in the biosorption yield of *T. elegans*. *p*-Values lower than 0.01 indicated that the variables were statistically significant.

3.2. Influence of process variables on RY2 biosorption performance

Fig. 1(a) showed the interactive effect of pH and biosorbent amount on the biosorption yield of the biosorbent. According to this figure, pH and biosorbent amount significantly effected the RY2 biosorption performance of *T. elegans*. The biosorption yield of the biosorbent increased by decreasing initial pH of the biosorption medium and increasing amount of the biosorbent. At acidic pH values, biosorbent surface positively charged due to the protonation of the functional groups on the biosorbent. Thus, electrostatic attraction forces between dye anions and positively charged biosorbent surface were predominate. On the other hand increasing pH caused a significant decrease in the biosorption yield of the biosorbent. This decrease may be attributed to the deprotonation of the functional groups on the biosorbent (Tian et al., 2010). These observations can also be explained by the zero point of charge (ZPC) (around pH 2.5) (Akar et al., 2013b) of the biosorbent.

An increase in the biosorbent amount also caused a significant increase in the biosorption potential of the biosorbent. This behavior could be explained by increasing number of available sites and larger surface area of the biosorbent with increasing biosorbent amount (Aksu and Çağatay, 2006).

The combined effect of pH and contact time on the biosorption of RY2 is indicated in Fig. 1(b). It is evident that the biosorption yield of the dye increased by increasing contact time. However, the biosorption yield of the biosorbent decreased by an increase in the pH.

Fig. 1(c) showed the combined effect of the biosorbent amount and contact time on the dye biosorption performance of *T. elegans*. Simultaneously, increasing amount of the biosorbent and longer contact time lead to an increase in the biosorption yield of the biosorbent as earlier.

3.3. Optimization of RY2 biosorption parameters

In order to obtain the maximum biosorption yield for RY2, operating parameters were optimized using quadratic model. Suggested optimum values of process variables are pH 2.0, biosorbent amount: 0.06 g and contact time: 39.3 min to reach maximum 99.42% RY2 removal yield. This predicted value was very close to the experimental value of 94.51%.

3.4. Biosorption kinetics

Contact time was varied from 5 to 60 min in order to investigate the kinetic parameters for the biosorption of RY2 onto *T. elegans* (Fig. 1(d)). The biosorption equilibrium was established within 40 min and this finding was agreed with the predicted value from quadratical model. The linear forms of the pseudo-first-order (Eq. (3)) and the pseudo-second-order (Eq. (4)) kinetic models were used to fit these data. The model constants and R^2 values are included in Table 1. This table indicated the time-dependent data were well fitted to the pseudo-second-order kinetic model with R^2 value of 0.999. The equilibrium biosorption capacity calculated from this model (74.61 mg g^{-1}) was also very close to the experimental value of 73.29 mg g^{-1}. On the other hand, R^2 value was not high and there is no consistence between experimental and calculated biosorption capacity values of the pseudo-first-order model. Consequently, the pseudo-second-order kinetic model appropriately described the kinetics and the chemisorption may be the main mechanism (Dragan et al., 2014) for RY2 biosorption in this study.

3.5. Biosorption isotherms

The Langmuir, Freundlich and D–R isotherms were tested to fit the equilibrium data for the biosorption of RY2 by *T. elegans* and the general isotherm plot is presented in Fig. 1(e). The calculated isotherm parameters and R^2 values are included in Table 1. Corresponding data indicated that the equilibrium data fit well with the Langmuir isotherm with the highest R^2 value (0.998). The Langmuir constants q_{max} and K_L were found to be 3.30×10^{-4} mol g^{-1} (288.08 mg g^{-1}) and 2.89×10^4 L mol^{-1}, respectively. The monolayer biosorption capacity of *T. elegans* is comparable with the literature values for RY2 decolorization with different biosorbent materials in Table 2 (Low et al., 1998; Aksu, 2001; Uzun, 2006; Akkaya et al., 2007; Hu et al., 2007; Al-Degs et al., 2008; Won and Yun, 2008). R_L value lying between 0 and 1 and *n* value between 1 and 10 are strong evidences for favorable biosorption of RY2. On the other hand, the magnitude of *E* value in this study (13.04 kJ mol^{-1}) indicated that the chemisorption based ion-exchange mechanism (Bhatt and Shah, 2015) may play a role in RY2 biosorption by *T. elegans*.

3.6. Column studies

Batch biosorption experiments represent fundamental information on the dye biosorption potential of a biosorbent (Vijayaraghavan and Yun, 2008b). But there is need to use these data for large scale industrial applications. Therefore, biosorption studies were also conducted in continuous system.

3.6.1. Effect of biosorbent amount

The effect of biosorbent amount on the biosorption of RY2 on *T. elegans* was also investigated in a continuous system at a flow rate of 1 mL min^{-1} and using dye solution (25 mL) at

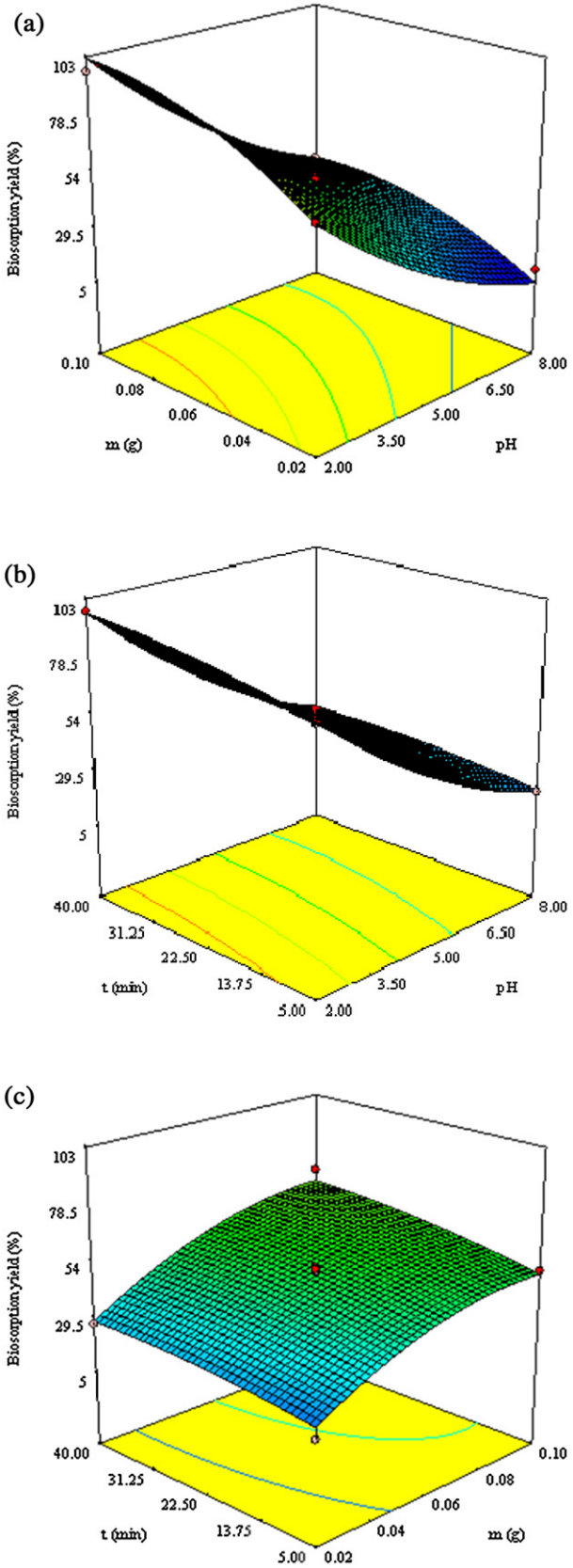

Fig. 1 – Response surface plots showing the effects of pH and biosorbent amount (a), pH and contact time (b), biosorbent amount and contact time (c), for the biosorption of RY2 onto *T. elegans*. Effect of contact time on the biosorption yield of RY2 onto *T. elegans* (d), general isotherm for the biosorption of RY2 onto *T. elegans* (e), effect of biosorbent amount on the biosorption yield of RY2 in continuous system (f), effect of flow rate on the biosorption yield and biosorption capacity of *T. elegans* in continuous system (g), consecutive biosorption–desorption cycles of *T. elegans* biomass (h), breakthrough curve for RY2 biosorption process (C: 100 mg L^{-1}; *m*: 40 mg; flow rate: 1.0 mL min^{-1}) (i).

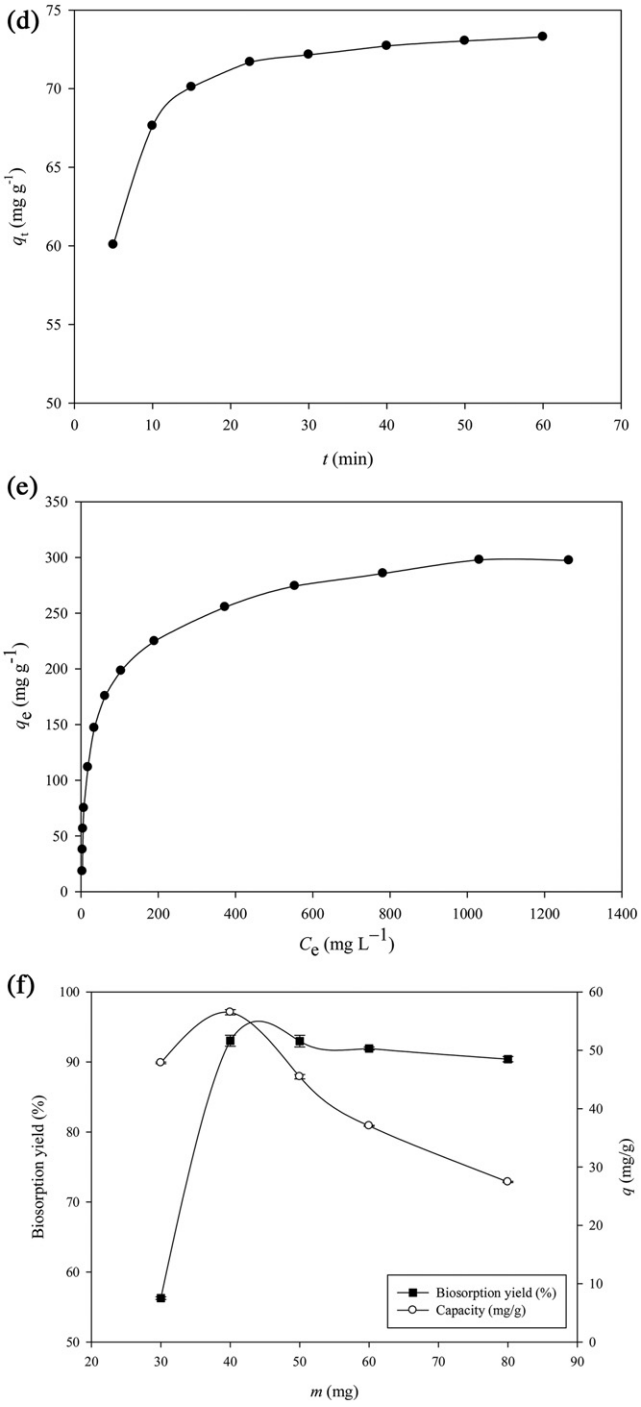

Fig. 1 – (*Continued*)

Table 1 – Kinetic and isotherm parameters for the biosorption of RY2 onto *T. elegans*.

Kinetic models									
Psuedo-first-order			Psuedo-second-order				Intraparticle diffusion		
k_1 (min^{-1})	q_e (mg g^{-1})	R^2	k_2 (g mg^{-1} min^{-1})	q_e (mg g^{-1})	h (mg g^{-1} min^{-1})	R^2	k_p (mg g^{-1} min^{-2})	C (mg g^{-1})	R^2
3.91×10^{-2}	5.94	0.618	1.28×10^{-2}	74.61	71.48	0.999	2.80	57.02	0.786
Isotherm models									
Freundlich			Langmuir				Dubinin–Radushkevich (D–R)		
n	K_F (L g^{-1})	R^2	q_{max} (mol g^{-1})	K_L (L mol^{-1})	$R_L{}^2$	R_L	q_m (mol g^{-1})	β (mol^2 kJ^{-2})	$R_{D-R}{}^2$
3.04	3.65×10^{-3}	0.895	3.30×10^{-4}	2.89×10^4	0.998	1.70×10^{-2}	8.75×10^{-4}	2.94×10^{-9}	0.934

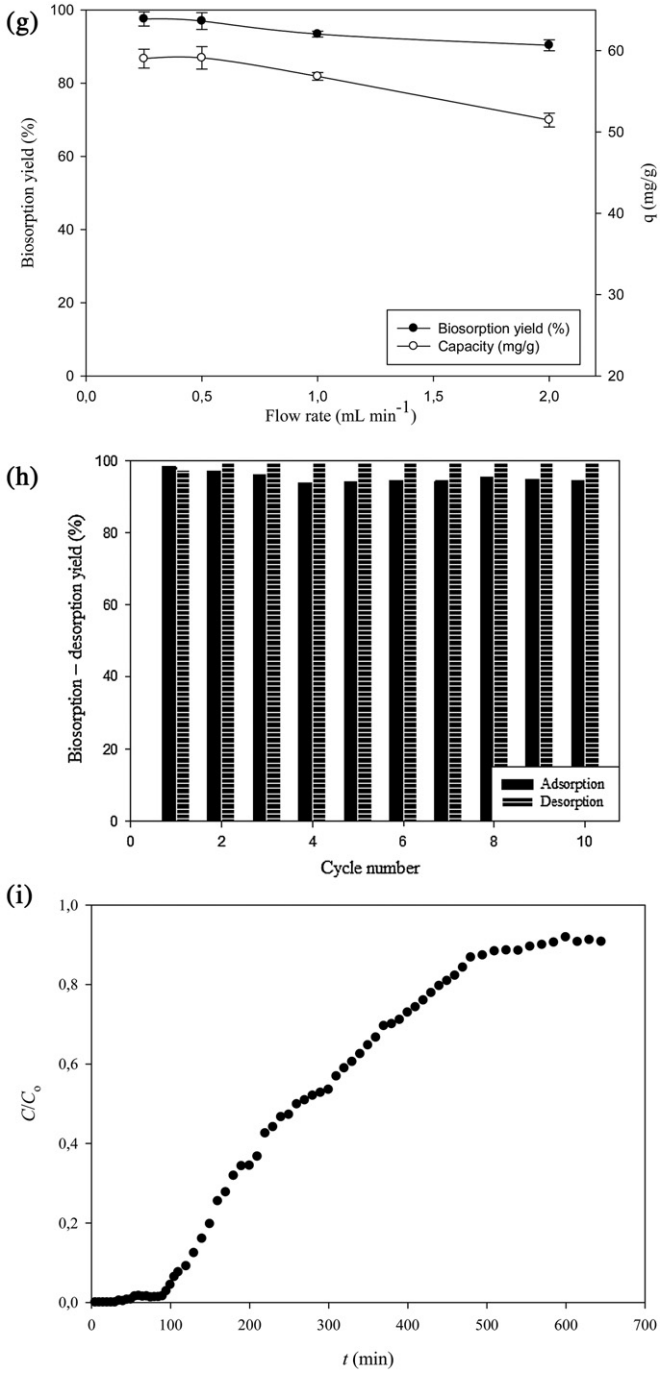

Fig. 1 – (*Continued*)

Table 2 – Biosorption results of RY2 by different sorbent materials from the literature.

Sorbent material	Sorption capacity (mg g^{-1})	References
Coconut husk	182.2	Low et al. (1998)
Dried activated sludge	333.3	Aksu (2001)
Chitosan	~75	Uzun (2006)
Chitin	~37	Akkaya et al. (2007)
Clay	61.8	Hu et al. (2007)
Activated carbon	209.4	Al-Degs et al. (2008)
Corynebacterium glutamicum	178.5	Won and Yun (2008)
T. elegans	288.08	This study

an initial concentration of 100 mg L^{-1} at pH 2.0. Fig. 1(f) indicated that the increase in the biosorbent amount filled into the column from 30 mg to 40 mg caused an increase in the biosorption yield from 56.27% to 93.03% ($p < 0.05$). The biosorption yield of *T. elegans* did not change with further increase in the biosorbent amount ($p > 0.05$). This trend may be explained by the increase in the bed height of the column with increasing biosorbent amount. Thus, dye solutions longer interact with biosorbent in the column.

5.6.2. *Effect of flow rate*

The results presented in Fig. 1(g) indicated the flow rate had considerable effect on the biosorption of RY2 on *T. elegans*. The maximum RY2 biosorption (97.55%) was occurred at a flow rate of 0.50 mL min^{-1}. When the flow rate was adjusted to lower values, dye solution had more time to contact with the biosorbent in the column. This behavior results in higher biosorption yield and indicates that the biosorption of RY2 on *T. elegans* at the flow rates of 0.25 and 0.50 mL min^{-1} is dominated by the diffusion across boundary layers on the biosorbent surface. When the solution comes into contact with a biosorbent the laminar flow is the predominant flow state. In contrast, biosorption yield of RY2 decreased at high flow rates due to turbulent flow. In this stage, the biosorption process dominantly takes place by the diffusion within the biosorbent micropores (Liu et al., 2013).

3.7. *Regeneration studies*

Desorption characteristics of the biosorbent were investigated to examine the interaction type between biosorbent and dye solution and to test the reuse potential of biosorbent. In the present study, 0.01 M KOH was used as extractor for RY2 dye. Fig. 1(h) indicated the biosorption and desorption potential of the biosorbent for 10 cycles. Almost complete regeneration of *T. elegans* was achieved during all desorption processes. Furthermore, biosorption potential of the biosorbent was not lost even at the end of 10th cycle (94.52%). These findings strongly indicated that *T. elegans* may be suitable for practical applications.

3.8. *Breakthrough study*

In order to examine the breakthrough behavior of *T. elegans*, 100 mg L^{-1} RY2 solution was passed through the column packed with 0.2 g of the biosorbent at a flow rate of 0.5 mL min^{-1}. The breakthrough curve for the biosorption of RY2 onto *T. elegans* is given in Fig. 1(i). The breakthrough point emerged around 300 min and reached to exhaustion after 600 min. The adsorption capacity and yield values of *T. elegans* were also calculated from the breakthrough curve and found as 57.38 mg and 44.82%, respectively. These data showed that *T. elegans* can be successfully used in column applications for the decolorization of RY2 containing solutions.

3.9. *Characterization of biosorbent*

In order to characterize the decolorization process, absorption spectra of wastewater before and after RY2 biosorption were taken. UV–vis spectra in Fig. 2(a) indicated that the significant intensity decrease in the absorption peak after the treatment of wastewater with the biosorbent. This finding is an important evidence for the removal of RY2 and other dyes present in the wastewater.

The chemical composition of *T. elegans* was investigated using elemental analysis. The percentages of nitrogen, carbon and hydrogen were found as 7.29, 42.62 and 6.48%, respectively. The BET surface area was determined as 10.76 m^2 g^{-1}.

The surface morphology of *T. elegans* and RY2 loaded *T. elegans* was studied by AFM technique. AFM images of the unloaded- and dye-loaded biosorbent are presented in Fig. 2(b). These images indicated that the biosorption of RY2 onto *T. elegans* caused some apparent changes on the biosorbent surface. The rough structure of the biosorbent sur-

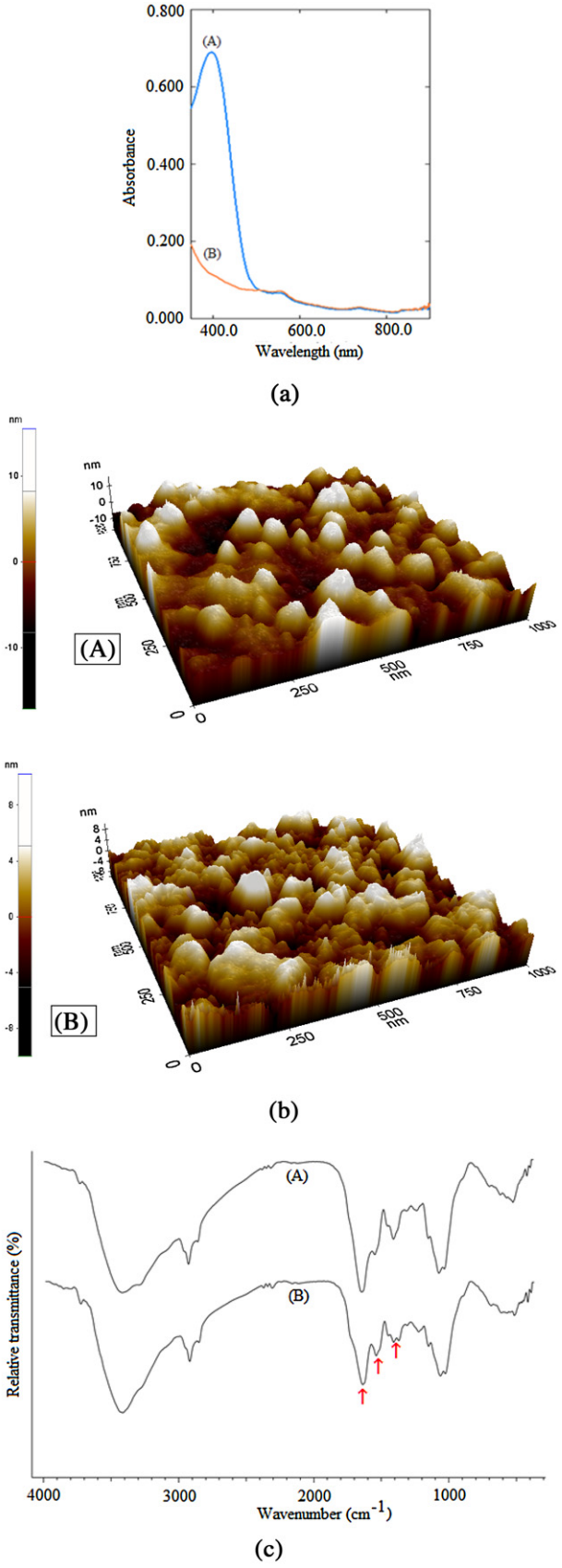

Fig. 2 – UV spectrum of wastewater before (A) and after (B) biosorption process (a), AFM images of *T. elegans* (A) and RY2 loaded *T. elegans* (B) (b) IR spectra of *T. elegans* (A) and RY2 loaded *T. elegans* (B) (c).

face converted into the irregular form. This finding was also explained by the biosorption of the dye onto *T. elegans*.

IR spectral analysis shows that the biomass prepared from *T. elegans* cells has a variety of functional groups, including –OH, –NH, $–CH_3$, CH_2, C=O, C–N, C–O–C, P–O and P–OH (Akar et al., 2013a). The role of these functional groups in the decolorization process was evaluated by comparing the spectra of raw and dye-loaded biosorbents (Fig. 2(c)). After contacting with dye solutions, the peaks at 1633 cm^{-1} (indicative of C=O stretching), 1325 cm^{-1} (indicative of C–H bending) and 1242 cm^{-1} (indicative of C–O–C stretching) and 1407 cm^{-1} (C–N stretching) were shifted to 1645, 1312, 1230 and 1416 cm^{-1}, respectively. Also an intensity decrease was observed for the last peak after the biosorption process. These results indicated that the mentioned groups are likely responsible for the biosorption of RY2 molecules onto biosorbent surface. Additionally, IR spectrum of dye-loaded *T. elegans* biomass exhibited new peaks at 1545 and 1377 cm^{-1} and they were attributed to –N=N– and C–N groups in dye structure, respectively. These differences between IR spectra of the biosorbent before and after the decolorization process may be strong evidences for the biosorption of RY2 onto *T. elegans*.

4. Conclusions

The present study indicated that biomass prepared from *T. elegans* cells was efficiently used for the biosorptive treatment of RY2 contaminated real wastewater with the excellent biosorption yields in both batch and column systems. pH, biosorbent amount and contact time were screened for the multivariate optimization of the treatment process. A quadratical model was suggested for the interpretation of the biosorption data with R^2 and F values of 0.986 and 56.90, respectively. Overall, this suggested biomaterial is a potential alternative for the wastewater decolorization with the fast biosorption rate, high biosorption capacity and excellent regeneration potential over 10 consecutive cycles.

Conflict of interest

The authors have declared no conflict of interest.

Appendix A. Supplementary data

Supplementary data associated with this article can be found, in the online version, at http://dx.doi.org/10.1016/j.psep.2016.11.017.

References

Akar, T., Arslan, S., Akar, S.T., 2013a. Utilization of *Thamnidium elegans* fungal culture in environmental cleanup: a reactive dye biosorption study. Ecol. Eng. 58, 363–370.

Akar, T., Kulcu, A., Akar, S.T., 2013b. Effective decolorization potential of *Thamnidium elegans*: biosorption optimization, modelling, characterization and application studies. Chem. Eng. J. 221, 461–468.

Akar, T., Turkyilmaz, S., Celik, S., Akar, S.T., 2016. Treatment design and characteristics of a biosorptive decolourization process by a green type sorbent. J. Clean. Prod. 112 (Part 5), 4844–4853.

Akkaya, G., Uzun, İ., Güzel, F., 2007. Kinetics of the adsorption of reactive dyes by chitin. Dyes Pigments 73, 168–177.

Aksu, Z., 2001. Biosorption of reactive dyes by dried activated sludge: equilibrium and kinetic modelling. Biochem. Eng. J. 7, 79–84.

Aksu, Z., Çağatay, Ş.Ş., 2006. Investigation of biosorption of Gemazol Turquise Blue-G reactive dye by dried *Rhizopus arrhizus* in batch and continuous systems. Sep. Purif. Technol. 48, 24–35.

Al-Degs, Y.S., El-Barghouthi, M.I., El-Sheikh, A.H., Walker, G.M., 2008. Effect of solution pH, ionic strength, and temperature on adsorption behavior of reactive dyes on activated carbon. Dyes Pigments 77, 16–23.

Allen, S.J., Koumanova, B., 2005. Decolourisation of water/wastewater using adsorption. J. Univ. Chem. Technol. Metall. 40, 175–192.

Bhatt, R.R., Shah, B.A., 2015. Sorption studies of heavy metal ions by salicylic acid-formaldehyde-catechol terpolymeric resin: isotherm, kinetic and thermodynamics. Arabian J. Chem. 8, 414–426.

Chatzifragkou, A., Makri, A., Belka, A., Bellou, S., Mavrou, M., Mastoridou, M., Mystrioti, P., Onjaro, G., Aggelis, G., Papanikolaou, S., 2011. Biotechnological conversions of biodiesel derived waste glycerol by yeast and fungal species. Energy 36, 1097–1108.

Chaudhary, N., Balomajumder, C., 2014. Optimization study of adsorption parameters for removal of phenol on aluminum impregnated fly ash using response surface methodology. J. Taiwan Inst. Chem. Eng. 45, 852–859.

Daneshvar, E., Vazirzadeh, A., Niazi, A., Sillanpää, M., Bhatnagar, A., 2017. A comparative study of methylene blue biosorption using different modified brown, red and green macroalgae — effect of pretreatment. Chem. Eng. J. 307, 435–446.

Dragan, E.S., Cocarta, A.I., Dinu, M.V., 2014. Facile fabrication of chitosan/poly(vinyl amine) composite beads with enhanced sorption of Cu^{2+}. Equilibrium, kinetics, and thermodynamics. Chem. Eng. J. 255, 659–669.

Dubinin, M., Radushkevich, L., 1947. Equation of the characteristic curve of activated charcoal. Chem. Zent. 1, 875–890.

Fakhri, A., 2015. Investigation of mercury (II) adsorption from aqueous solution onto copper oxide nanoparticles: optimization using response surface methodology. Process Saf. Environ. Prot. 93, 1–8.

Fernandez, M.E., Nunell, G.V., Bonelli, P.R., Cukierman, A.L., 2012. Batch and dynamic biosorption of basic dyes from binary solutions by alkaline-treated cypress cone chips. Bioresour. Technol. 106, 55–62.

Fomina, M., Gadd, G.M., 2014. Biosorption: current perspectives on concept, definition and application. Bioresour. Technol. 160, 3–14.

Fontana, K.B., Chaves, E.S., Sanchez, J.D.S., Watanabe, E.R.L.R., Pietrobelli, J.M.T.A., Lenzi, G.G., 2016. Textile dye removal from aqueous solutions by malt bagasse: isotherm, kinetic and thermodynamic studies. Ecotoxicol. Environ. Saf. 124, 329–336.

Freundlich, H., 1906. Über die absorption in lösungen. Universität Leipzig, 98 pp.

Hall, K.R., Eagleton, L.C., Acrivos, A., Vermeulen, T., 1966. Pore- and solid-diffusion kinetics in fixed-bed adsorption under constant pattern conditions. Ind. Eng. Chem. Fundam. 5, 212–223.

Hasan, S.H., Ranjan, D., Talat, M., 2009. "Rice Polish" for the removal of arsenic from aqueous solution: optimization of process variables. Ind. Eng. Chem. Res. 48, 4194–4201.

Ho, Y.-S., 2006. Review of second-order models for adsorption systems. J. Hazard. Mater. 136, 681–689.

Hu, Q., Xu, Z., Qiao, S., Haghseresht, F., Wilson, M., Lu, G.Q., 2007. A novel color removal adsorbent from heterocoagulation of cationic and anionic clays. J. Colloid Interface Sci. 308, 191–199.

Kuhnt, M., Bitsch, F., Ponelle, M., Fehr, T., Sanglier, J.-J., 1997. Microbial conversion of rapamycin. Enzyme Microb. Technol. 21, 405–412.

Kuyucak, N., 1990. Feasibility of biosorbents application. In: B, V. (Ed.), Biosorption of Heavy Metals. CRC Press, Boca Raton, Florida, pp. 372–377.

Lagergren, S., 1989. Zur theorie der sogenannten adsorption gelöster stoffe, Kungliga Svenska Vetenskapsakademiens. Handlingar 24, 1–39.
Langmuir, I., 1918. The adsorption of gases on plane surfaces of glass, mica and platinum. J. Am. Chem. Soc. 40, 1361–1403.
Lee, L.Y., Gan, S., Yin Tan, M.S., Lim, S.S., Lee, X.J., Lam, Y.F., 2016. Effective removal of Acid Blue 113 dye using overripe *Cucumis sativus* peel as an eco-friendly biosorbent from agricultural residue. J. Clean. Prod. 113, 194–203.
Liu, W., Zhao, Z., Guo, Y., 2013. Removal of lead ions from ginseng ethanol extracts by dynamic adsorption in a fixed-bed column. Chin. J. Chem. Eng. 21, 227–231.
Low, K.S., Lee, C.K., Lee, K.L., 1998. Removal of reactive dyes by quaternized coconut husk. J. Environ. Sci. Health 33 (Part A), 1479–1489.
Murugesan, A., Vidhyadevi, T., Kalaivani, S.S., Thiruvengadaravi, K.V., Ravikumar, L., Anuradha, C.D., Sivanesan, S., 2014. Modelling of lead(II) ion adsorption onto poly(thiourea imine) functionalized chelating resin using response surface methodology (RSM). J. Water Process Eng. 3, 132–143.
Nath, J., Ray, L., Bera, D., 2016. Continuous removal of malachite green by calcium alginate immobilized *Bacillus cereus* M116 in packed bed column. Environ. Technol. Innov. 6, 132–140.
Solís, M., Solís, A., Pérez, H.I., Manjarrez, N., Flores, M., 2012. Microbial decolouration of azo dyes: a review. Process Biochem. 47, 1723–1748.
Stredansky, M., Conti, E., Stredanska, S., Zanetti, F., 2000. γ-Linolenic acid production with *Thamnidium elegans* by solid-state fermentation on apple pomace. Bioresour. Technol. 73, 41–45.
Tian, Y., Ji, C., Zhao, M., Xu, M., Zhang, Y., Wang, R., 2010. Preparation and characterization of baker's yeast modified by nano-Fe_3O_4: application of biosorption of methyl violet in aqueous solution. Chem. Eng. J. 165, 474–481.
Tigini, V., Prigione, V., Donelli, I., Anastasi, A., Isella, F., Freddi, G., Varese, G.C., 2011. Fungal biomasses: non conventional biosorbents for organic and inorganic pollutants. In: Crini, G., Badot, P.-M. (Eds.), Sorption Processes and Pollution: Conventional and Non-conventional Sorbents for Pollutant Removal from Wastemasters. Presses Universitaires de Franche-Comté, pp. 359–384.
Tunali Akar, S., Gorgulu, A., Akar, T., Celik, S., 2011. Decolorization of Reactive Blue 49 contaminated solutions by *Capsicum annuum* seeds: batch and continuous mode biosorption applications. Chem. Eng. J. 168, 125–133.
Uzun, İ., 2006. Kinetics of the adsorption of reactive dyes by chitosan. Dyes Pigments 70, 76–83.
Vijayaraghavan, K., Yun, Y.-S., 2008a. Bacterial biosorbents and biosorption. Biotechnol. Adv. 26, 266–291.
Vijayaraghavan, K., Yun, Y.-S., 2008b. Biosorption of C.I. Reactive Black 5 from aqueous solution using acid-treated biomass of brown seaweed *Laminaria* sp. Dyes Pigments 76, 726–732.
Won, S.W., Yun, Y.-S., 2008. Biosorptive removal of Reactive Yellow 2 using waste biomass from lysine fermentation process. Dyes Pigments 76, 502–507.

Update

Process Safety and Environmental Protection

Volume 111, Issue , October 2017, Page 810

DOI: https://doi.org/10.1016/j.psep.2017.08.020

Contents lists available at ScienceDirect

Process Safety and Environmental Protection

journal homepage: www.elsevier.com/locate/psep

Corrigendum

Corrigendum to "The feasibility of *Thamnidium elegans* cells for color removal from real wastewater" [Process Saf. Environ. Prot. 105 (2017) 316–325]

Tamer Akar[a,*], *Fatih Sayin*[a], *Serpil Turkyilmaz*[b], *Sibel Tunali Akar*[a]

[a] *Department of Chemistry, Faculty of Arts and Science, Eskişehir Osmangazi University, Turkey*
[b] *Department of Statistics, Faculty of Arts and Science, Bilecik Şeyh Edebali University, 11210 Bilecik, Turkey*

The authors of the above mentioned article regret they mistakenly did not include an acknowledgement section for financial support of our institute. The acknowledgement section should have read as follows:

The authors are thankful to Eskisehir Osmangazi University (ESOGU) for the financial support. This work was supported by Commission of Scientific Research Projects of ESOGU (project no.: 201519D07).

The authors would like to apologise for any inconvenience caused.

DOI of original article:http://dx.doi.org/10.1016/j.psep.2016.11.017.
* *Corresponding author*.
E-mail address: takar@ogu.edu.tr (T. Akar).
http://dx.doi.org/10.1016/j.psep.2017.08.020